



Research paper

Enhancement of mechanical properties of concrete using microwave cured bamboo composites

Ajayi Joseph Adeniyi¹, James Gana², Ariyo Adanikin³,
Kola Ogedengbe⁴, Abundance Idowu⁵

Abstract: Microwave curing of bamboo fiber increases the physical and mechanical qualities of cement concrete, according to previous studies. However, there are limited research on their endurance when used as an additive in concrete manufacturing to increase strength. The impact of bamboo fiber and Styrene Butadiene Rubber (SBR) on the mechanical and microstructure of the resulting concrete is investigated in this study. With the inclusion of bamboo fiber ranging from 0–1.5%, a mix ratio of 1:1.5:3 was used. To make the samples, 10% SBR by weight of cement was dissolved in the mixing water. The batching was done by weight, with a water cement ratio of 0.6. Compressive strength, water absorption, swelling, modulus of elasticity, and modulus of rupture were all studied as mechanical properties. Various characterization tests such as SEM, EDS, FTIR, XRD, and TGA were performed on the microstructure, crystalline nature, and mineral composition of certain samples. According to the FTIR study's findings, peak levels were detected in the O–H stretching, C–H fiber and CH₂ functional groups, carbonyl group, C–O and C–C functional groups. As the temperature climbed, TGA measurements showed a drop in weight. The XRD test revealed peak levels of 6.611, 4.255, and 3.855 for sanidine, quartz, and calcite, respectively. After 28 days, the inclusion of bamboo fibers as an additive in concrete shows some promising outcomes in compressive strength, with samples containing 1% and 1.5% bamboo fiber cured at 80°C having a higher compressive strength value.

Keywords: bamboo fiber, compressive strength, microwave curing, modulus of rupture, swelling, styrene butadiene rubber

¹PhD., Eng., Landmark University, School of Engineering, Department of Civil Engineering, Omu-Aran, Kwara State, Nigeria, e-mail: ajayi.joseph@lmu.edu.ng, ORCID: 0000-0001-6424-1207

²PhD., Eng., Landmark University, School of Engineering, Department of Civil Engineering, Omu-Aran, Kwara State, Nigeria, e-mail: gana.abu@lmu.edu.ng, ORCID: 0000-0001-9122-2490

³PhD., Eng., Elizade University, Faculty of Engineering, Dept. of Civil Engineering, Ilara mokin, Ondo State, Nigeria, e-mail: ariyo.adanikin@elizadeuniversity.edu.ng, ORCID: 0000-0001-8455-1202

⁴PhD., Eng., Landmark University, School of Engineering, Department of Civil Engineering, Omu-Aran, Kwara State, Nigeria, e-mail: kolaogedengbe@yahoo.com, ORCID: 0000-0002-3873-913X

⁵B. Eng., Landmark University, School of Engineering, Department of Civil Engineering, Omu-Aran, Kwara State, Nigeria, e-mail: abundanceid00@gmail.com, ORCID: 0000-0002-3098-9740

1. Introduction

Bamboo fiber is present naturally in bamboo trees and can be isolated using a variety of methods and procedures. Bamboo has two strategies for arranging vegetative axes that are commonly sorted out: one is above ground, and the other is below ground [1]. When climatic conditions change, bamboo's mechanical qualities may change [2]. The fibers can only be segregated into Bamboo pulp fiber or original bamboo strands, regardless of the method utilized. The strands of original bamboo fiber are clearly ejected from the original bamboo utilizing chemical and physical procedures without the use of chemicals [2]. The bamboo is first treated with alkali hydrolysis (NaOH) to produce cellulose fibers [3]. Bamboo is an environmentally friendly conventional fiber with a fast growth rate that aids in the removal of carbon dioxide from the atmosphere; these biological properties make it the most important plant fiber [4]. The accelerated aging test is a test that can provide insight into the mechanism at the microstructure level [5]. Accelerated aging tests reveal a material's long-term behavior as a result of biological or environmental factors.

Microwave curing has been shown to be a faster and more effective way for enhancing compressive strength, porosity, and composition than traditional heat curing. Microwaves are utilized in material processing, such as curing laminate adhesives, and microwave curing is being employed in experiments to enhance the hydration of solid paste, resulting in increased strength. Chemical accelerators (such as calcium chloride, CaCl) used in the strength development of concrete have been shown to alter the concrete's longevity, particularly when reinforced with steel [6]. As a result, this study looks at enhancing the mechanical properties of concrete using bamboo fiber as admixture and microwave curing as means of curing of the cubes.

2. Materials and methods

Table 1 presents information on the type and sources of materials used for this study.

Table 1. The sources of Materials used

Materials	Source
Bamboo culm	Landmark university commercial farm
Fine aggregate	Landmark university concrete shed
Portland cement	A cement dealer in Omu-Aran market
Styrene butadiene Rubber	A chemical dealer in Lagos
Calcium Chloride	A chemical dealer in Lagos
Sodium Hydroxide	A chemical dealer in Lagos

2.1. Preparation of bamboo fibre

The bamboo was cut at the nodes and broken to small splints as shown in Fig. 1. Thereafter, the bamboo splints were air dried for 3 days to reduce the moisture content. It was dried further in the oven for 24 hours at a temperature at 80°C. The bamboo splints as shown in Fig. 2, were taken to a hammer mill and were milled into fibres. The fibre was sieved manually using 2.00 mm sieve and the retained are used for this research.



Fig. 1. Bamboo splints



Fig. 2. Hammer mill used

2.2. Chemical treatment of fibre

The chemical used for the treatment was sodium hydroxide (NaOH). The bamboo fibres were soaked in a solution of NaOH with a concentration of 30% for 24 hrs. Afterwards, it was washed severally in water to remove the chemicals and make the fibre pure. The treated fibre as shown in Fig. 3 was spread out on a flat surface and left to air dry for 24 hrs.



Fig. 3. Sieving of the fiber

2.3. Mix formation

The mix design comprises of variations in quantity of bamboo fiber and Styrene Butadiene Polymer (SBR) used as the modifier. CaCl₂ (as partial replacement of 3% of cement) was used which served as an accelerator to stabilize the bamboo fiber and ensure it does not decompose. The mix ratio used was 1:1.5:3 and remained constant throughout the

experiment. A percentage of bamboo fiber ranging from 1–1.5 was added and vigorously mixed until the mixture was homogeneous. SBR (10% cement weight) was dissolved in water and added to the mix. The slurry was placed into a $300 \times 3000 \times 30 \text{ mm}^3$ mould and $150 \times 150 \text{ mm}^2$ compressive testing mould. Table 2 gives the experimental design for the mix. A total number of 144 samples were produced for all the categories and were tested at 7, 14, 21, and 28 days.

Table 2. Experimental design

Curing Regime	Sample no.	Bamboo fiber (%)	SBR (%)	Cement	Sand	Coarse aggregate	Replicates
Low Microwave Regime	DK 1	0	0	1	1.5	3	3
	DK 2	1	0	1	1.5	3	3
	DK 3	1.5	0	1	1.5	3	3
	DK 4	0	10	1	1.5	3	3
	DK 5	1	10	1	1.5	3	3
	DK6	1.5	10	1	1.5	3	3
Medium Microwave Regime	DK 7	0	0	1	1.5	3	3
	DK 8	1	0	1	1.5	3	3
	DK 9	1.5	0	1	1.5	3	3
	DK 10	0	10	1	1.5	3	3
	DK 11	1	10	1	1.5	3	3
	DK 12	1.5	10	1	1.5	3	3

2.4. Curing of sample

The microwave curing method and standard water curing method were employed in this research. The low microwave medium was set at 35 degrees Celsius, while the high microwave medium was set at 80 degrees Celsius. The samples were placed in the microwave with even spacing in both curing mediums to permit the heat waves to travel through the samples. The samples were heated for 1 hour in the microwave. The cubes were taken for the compressive test after they had been cured. Some flexural samples were utilized in the accelerated aging test, while the rest were packed in an airtight bag and cured in water for 28 days before being examined without the accelerated aging test to compare results.

2.5. Wet-dry accelerated aging cycle

The sample was subjected to wet and dry cycles during the accelerated aging test in order to determine the impact of environmental conditions that the fiber reinforced material will face in real-world applications. The test was carried out in compliance with the [7]. In the course of this study, 200 aging cycles (50 days of accelerated aging) were completed.

2.6. Mechanical properties

2.6.1. Water absorption

The goal of water adsorption is to determine each sample's dimensional stability. The samples were soaked for 2 hours and 24 hours in water, and the results were calculated using a standard formula.

2.6.2. Thickness swelling

The effect of water absorption on the thickness of the material was determined using thickness swelling. The samples were soaked in water for 2 hours and 24 hours at room temperature before being measured with a digital vernier caliper. The thickness swelling was calculated using Eq. (2.1).

$$(2.1) \quad TS = \frac{T_2 - T_1}{T_1} \cdot 100$$

where TS – thickness swelling (%), T_1 – initial thickness and T_2 – final thickness (after soaking).

2.6.3. Compressive test strength

This test was performed in the Landmark University concrete testing laboratory using a Universal testing machine (UTM) in compliance with [8].

2.6.4. Modulus of Rupture (MOR) and Modulus of Elasticity (MOE)

The MOE/MOR was completed in accordance with [9]. In a total of three replicates, the samples were loaded at a rate of 1.5 mm/min until failure occurred. Eq. (2.2) and (2.3) were used to determine the MOE and MOR, respectively.

$$(2.2) \quad MOE = \frac{4P_b}{4byh} L^3$$

$$(2.3) \quad MOR = \frac{3PL}{2bh^2}$$

where: MOR – modulus of rupture (N/mm²), MOE – modulus of elasticity (N/mm²), P – maximum loading force (N), P_b – load at proportional limit (N), L – span (mm), h – thickness of sample (mm) and y – deflection corresponding to P_b (mm).

2.7. Characterization test

The characterizations carried out on the sample in this study are scanning electron microscope/energy with dispersive X-ray (SEM/EDS) and thermal gravimetric analysis (TGA).

2.7.1. Scanning electron microscope / energy with dispersive X-ray (SEM/EDS)

After microwave curing, the fragmented samples were polished and analyzed using a field emission scanning electron microscope (FESEM) at a magnification range of $330\times$ to $750\times$ and a 15 kV acceleration voltage. Using a sputter, a thin layer of platinum was applied to the polished samples. For the four most important composites, a total of three SEM micrographs were collected, and photographs of the microstructure observed are shown in this study.

2.7.2. Thermal gravimetric analysis (TGD)

Thermal stability and fraction of volatile component of fractured samples would be tested after 28 days of curing. This is accomplished by utilizing a TGA analyzer to track the weight change that occurs on the samples while they are heated at a constant rate.

2.7.3. Fourier-transform infrared spectroscopy (FTIR)

The samples' functioning was determined using FTIR spectra after the 28-day test. The materials were crushed to a powder, which was then combined with potassium bromide powder and compacted in a disk. The samples' spectra were recorded. Table 3 gives the functional groups.

Table 3. Functional groups in samples

Wave Number (cm^{-1})		
DK6	DK12	Functional groups
3423.76	8448.84	OH groups
2928.04	2874.03	C-H
1871.01	2000.25	C=O
1793.86	195.79	C-O and C-C
1637.62	1635.69	C-O
468.72	459.07	V4 stretching of Si-O

2.7.4. X-ray Diffraction Analysis (XRD)

The mineral composition of a material, as well as the primary phases in the composite and the number of crystalline phases found, are determined using XRD. Using an XRD diffractometer, the different crystalline phases in the material were determined.

3. Results and discussion

3.1. Water absorption

Figure 4 shows the water absorption findings after 2 hours and 24 hours. As shown in Fig. 4, sample DK6 had the lowest water absorption rate of 5.29 percent, followed by DK1,

DK11, DK3, DK4, DK5, DK8, DK2, DK12, DK10, DK7, and DK9. DK9 had the highest water absorption rate of 9.90% after 24 hours. DK6 had the lowest percentage of water absorption at 4.92 after 2 hours, followed by DK3, DK11, DK8, DK4, DK12, DK10, DK5, DK2, DK7, and DK9, which had the highest percentage of water absorption at 9.49%. As revealed by [10–12] in analyzing the compressive strength and water absorption of styrene rubber in concrete, this is due to the creation of a polymer layer that makes the concrete water tight. After 24 hours, samples containing 1% and 1.5% fiber showed an increase in water absorption.

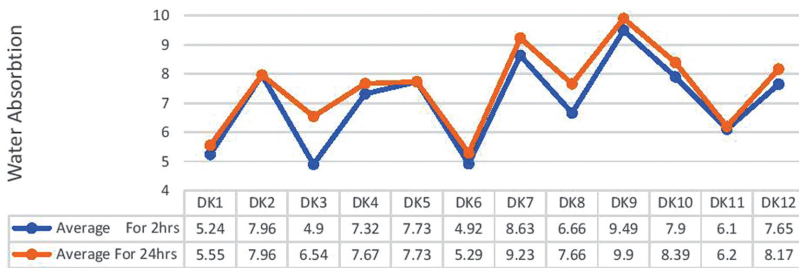


Fig. 4. Result of water absorption test

3.2. Thickness swelling

Figure 5 shows the findings of the Thickness Swelling for 2 hours and 24 hours. After 24 hours, DK7 had the lowest percentage of thickness swelling (1.97%), followed by DK5, DK3, DK1, DK10, DK11, DK9, DK8, DK2, DK12, DK6, and DK4 with the highest percentage of thickness swelling (11.94%). DK7 had the lowest percentage thickness swelling of 1.65 after 2 hours, followed by DK2, DK5, DK11, DK3, DK1, DK10, DK8, DK9, DK4, DK6, and DK12. DK12 had the highest percentage thickness swelling of 7.83% after 2 hours. As can be seen in Figure 4, there was a significant increase in thickness swelling as time passed. Water absorption and thickness swelling in polymeric

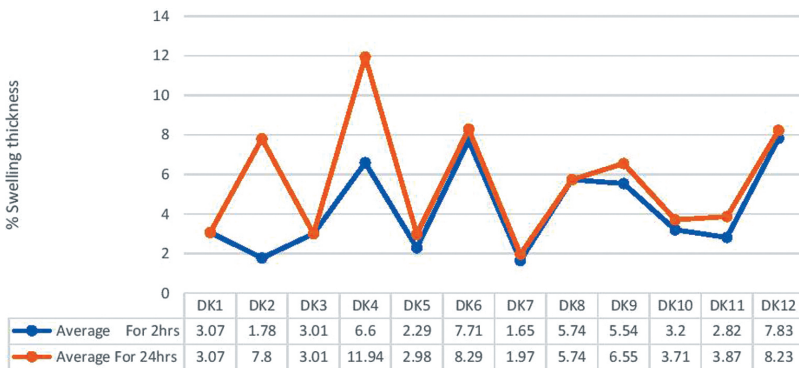


Fig. 5. Percentage thickness swelling for different samples

composite materials were evaluated by [13], and the results were consistent. Thickness swelling rises with time, until observable definite thickness swelling is noticed, according to their findings.

3.3. Compressive strength

Figure 6 depicts the results of the compressive strength test after 28 days of curing. The maximum compressive strength was 32.72 N/mm² for DK5, which contained 1% fiber and 10% SBR and was cured with a low microwave regime of 35°C. The lowest observable compressive strength was 21.04 N/mm² in DK1, which had a composition of 0% fiber and 0% SBR and was cured at 35°C. Samples cured with a medium regime of 80°C and having 1% and 1.5% fiber had a higher compressive strength than samples containing 0% fiber and cured with a low curing medium of 35°C, according to the results. In comparison to four other curing procedures, microwave curing produced the greatest increase in compressive strength, according to [14].

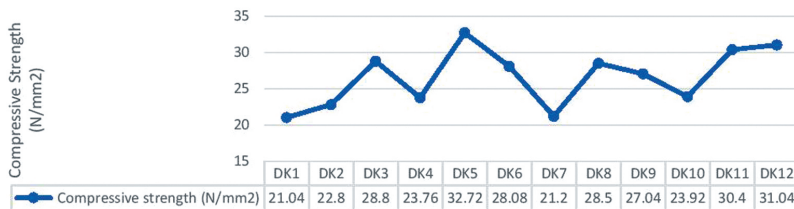


Fig. 6. Compressive strength value for different samples

3.4. Effect of water curing on Modulus of Rupture (MOR) & Modulus of Elasticity (MOE)

Fig. 7 and Fig. 8 show the findings of the MOE and MOR after 28 days of curing. The modulus of rupture ranged from 3.796 N/mm² to 6.957 N/mm² on average. DK10

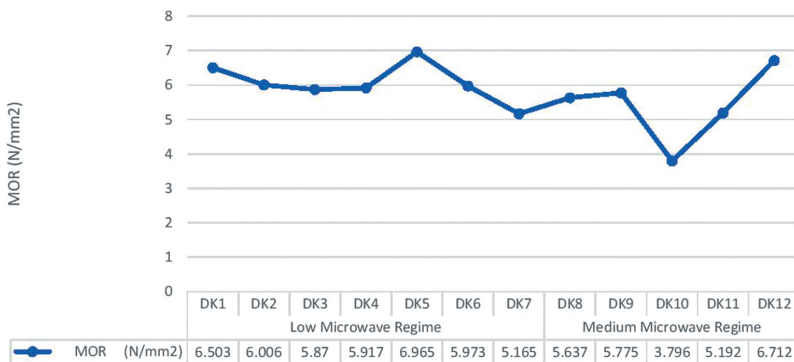


Fig. 7. Result of MOR after 28 days of curing

had the lowest Modulus of rupture of 3.796 N/mm², followed by DK7, DK11, DK8, DK9, DK3, DK4, DK2, DK6, DK1, DK12, and DK5 had the highest Modulus of rupture of 6.965 N/mm². According to the findings, samples containing 1% to 1.5% fiber had a higher modulus of rupture than samples containing 0% fiber. In their study of synergic impact treatments for matrix treatments vegetable fiber reinforced cement, [15] discovered the same thing. On samples reinforced with treated pulps, a 5% rise was recorded.

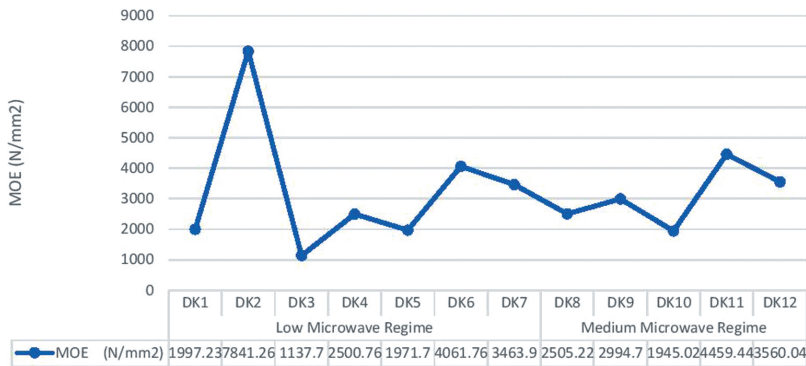


Fig. 8. Result of MOE after 28 days of curing

3.5. Result of modulus of rupture (MOR) and modulus of elasticity

Figure 9 shows that samples containing 1% to 1.5% fiber and 10% SBR had a considerable rise in MOR. After the accelerated aging test, sample DK5 (containing 1% fiber and 10% SBR) exhibited a 50% rise. After the accelerated aging test, sample Dk6 (made of 1.5% fiber and 10% SER) showed a 10% increase in MOR. After the accelerated aging test, MOR increased by 10% in Sample DK 11 (which contains 1% fiber and 10% SBR). MOR was improved in sample DK11 (which contained 1% fiber and 10% SBR). MOR improved by 10% in sample DK12 (made of 1.5% fiber and 10% SBR). The presence of

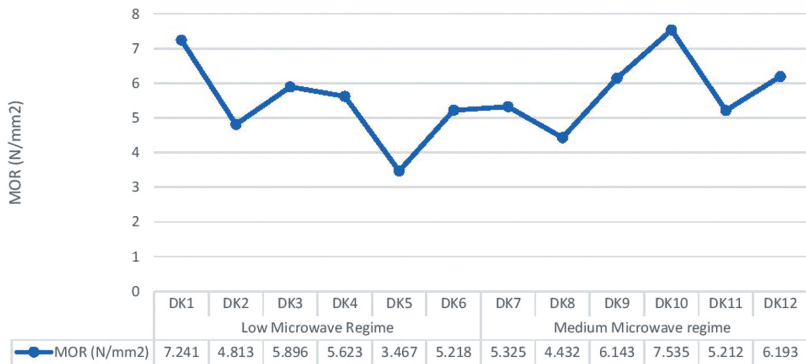


Fig. 9. Result of MOR after accelerated aging

SBR in the samples could explain the observed rise in MOR. In their study of the influence of experimental wet and dry cycles on bamboo fiber reinforced acrylic polymer modified cement composites, [16, 17] discovered a similar increase in MOR. The addition of polymer admixtures improved the microstructure of the composites, limiting the increase and enlargement of holes and voids during the wet and dry cycles, according to their findings. Figure 10 compares the modulus of elasticity of samples that were soaked for 28 days with samples that were aged more quickly. In samples containing 1% to 1.5% fiber, MOE was found to be lower. Samples DK5 had a 50% decrease in MOE, samples DK6 had a 15% decrease in MOE, sample DK11 had a 10% decrease in MOE, and samples DK12 had a 5% decrease in MOE. MOE values did not increase, but rather decreased, which could be due to the low concentration of extractives [18, 19].

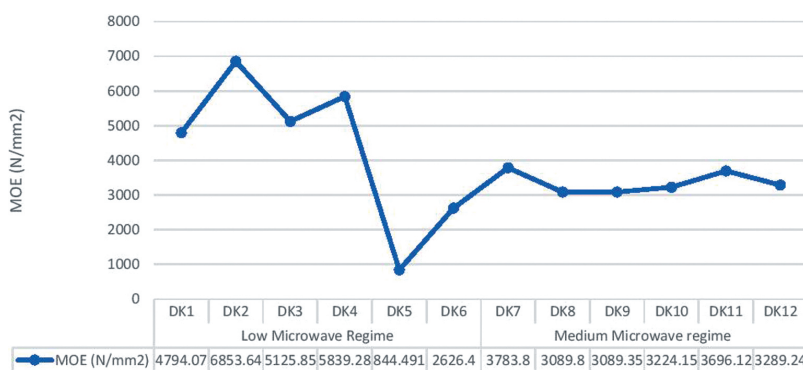


Fig. 10. Result of MOE after accelerated aging

3.6. Fourier-transform infrared spectroscopy (FTIR)

Fig. 11 and Fig. 12 show the FTIR spectroscopy results for sample DK6 cured at 35°C and DK12 cured at 80°C, respectively, while Table 2 shows the functional group. The fre-

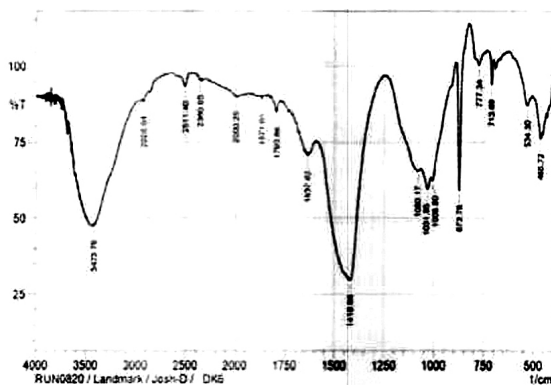


Fig. 11. Result FTIR spectra for sample DK6

quency band peaked at 3423 cm^{-1} in the FTIR graph in figure 12 which represented O–H stretching. C–H fiber and CH₂ groups are represented by the spectra bands at 2928.04 cm^{-1} and 2511.40 cm^{-1} , respectively. Carbonyl groups are represented by transmittance maxima at 2000.25 , 1871.0 , and 1637.62 cm^{-1} . Function groups of C–O and C–C are represented by the spectra bands at 14419.66 , 17 , and 1008.80 cm^{-1} . The bending functional groups SiO₄/RCH=CH₂ are represented by spectra bands spanning from 873.78 to 468 . The frequency spectrum peaked at 3449.84 cm^{-1} , indicating that O–H was stretched, whereas the spectra bands at 2874.03 cm^{-1} and 2513.3340 cm^{-1} represented C–H fiber and CH₂ groups, respectively. Carbonyl groups were represented by transmittance peaks at 2000.25 , 1795.79 , and 1635.69 cm^{-1} . The properties of function groups C–O and C–C were represented by the spectra band at 1423.51 , 1080.17 , and 1033.88 cm^{-1} . The bending functional groups SiO₄/RCH=CH₂ are represented by spectra bands spanning from 873.78 to 459.07 .

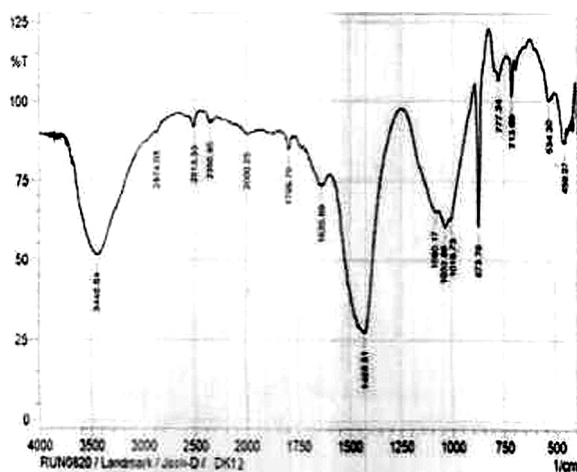


Fig. 12. Result spectra for sample DK12

3.7. Thermal gravimetric analysis (TGH)

The efficiency of the carbonation reaction can be determined using differential thermogravimetric analysis (DTA) [20–22]. The weight fluctuations were documented and graphed. DK6, which was made up of 1.5 percent fiber and 10% SBR and cured at 35 degrees Celsius had a steady weight loss when the temperature was raised from 200°C to 300°C . As the temperature rose to 500°C , the weight began to decline gradually. Between temperatures of 500°C and 884.1°C , the fast weight loss slowed. Sample DK12, which contained 1.5% fiber and 10% SBR and cured at 80°C also had a steady weight loss. As the temperature increased from 300°C to 500°C , a rapid loss of weight was noticed. When temperatures between 500°C and 883.6°C were reached, the rapid weight loss began to slow down.

3.8. X-ray diffraction analysis (XRD)

The mineral composition of DK6 which contained 1.5% fiber and 10% SR and cured in a low microwave regime of 35°C, was found to have a good percentage of quartz (silicon dioxide, SiO₂), portlandite (calcium hydroxide, Ca(OH)₂), and calcite (Calcium carbonate, CaCO₃) as shown in Table 4. The mineral composition for DK12, which contained 1.5% fiber and 10% SBR and was cured in a medium microwave regime of 80°C, had a great percentage of quartz (silicon dioxide, SiO₂), Calcite with sanidine (potassium feldspar, K(AlSi₃O₈) and calcium carbonate, (Ca) as presented in Table 5.

Table 4. XRD Results for DK6

Values obtained		
Portlandite	Quartz	Calcite
4.880	4.254	3.854

Table 5. XRD Results for DK12

Values obtained		
Sanidine	Quartz	Calcite
6.661	4.255	3.855

3.9. Scanning electron microscope/energy with dispersive X-ray (SEM/EDS)

The composites' microscopes were analyzed with the help of a scanning electron microscope. The fiber content of the samples chosen was between 1% and 1.5%. Back-scattered electron imaging mode can be used to create the micrographs (BSD) [23–25]. All of the photos have a 15 kV accelerating voltage with magnifications ranging from 812 μm to 822 μm. Images of four composites with varied fiber percentages and curing regimes are exhibited in SEM micrographs. The EDS analysis result revealed that, at a magnification of 813 μm for sample DK6 with a composition of 1.5% fiber and 10% SBR cured in a low microwave regime of 35°C, a high peak value of Ca (Calcium), Si (Silicon), and Y (Yttrium) (Yttrium) was observed. The result revealed that at a magnification of 812 μm for both sample DK9 and sample DK12, which were cured in a medium microwave regime of 80°C with a composition of 1% fiber and 10% SBR, high peak values of Ca (Calcium), Si (Silicon), and Y (Yttrium) were noted.

This study's findings are consistent with those of [26], which show a balanced microstructure before and after the addition of Styrene Butadiene Rubber (SBR). The results also revealed that the workability and density of the concrete improved with the addition of SBR. This is also consistent with the findings of [27], which show that curing mediums impact the microstructure of concrete and that the interfacial transition zones under different

curing regimes affect its compact nature. Furthermore, the findings of [28] show that adding SBR, which has filling and compacting properties, improves concrete properties by improving anti-freezing ability, creating cement hydration products like calcium silicate hydrates (C–S–H) and ettringite (Aft), coating aggregate particles, and the SBR polymer and cement hydration products bonding together to create an interpenetrating matrices that improves strength and microstructural ability of concrete in tandem with the findings of this study.

4. Conclusions

The addition of bamboo fibers as admixture in concrete productions show some encouraging results. The compressive strength comparison between them and the control samples at 28 days, showed increased in the compressive strength values. The maximum compressive strength was 32.72 N/mm² for DK5, which contained 1% fiber and 10% SBR and was cured in a low microwave regime of 35°C while the control sample (DK1) turned in the lowest compressive strength of 21.04 N/mm². It can therefore be concluded from the research that samples cured in a medium regime of 80°C and having 1% and 1.5% fiber had higher compressive strength values than samples containing 0% fiber and cured with a low curing medium of 35°C. The modulus of rupture increased as the wet and dry cycles progressed. A recommended value of 18 N/mm² for modulus of rupture and 3000 N/mm² for modulus of elasticity are allowed for structural purposes; nevertheless, a few samples were within the standard limits for modulus of elasticity. The measurements for water absorption and thickness swelling are within permissible limits.

Acknowledgements

The authors are grateful to Civil Engineering department, College of Engineering, Landmark University, Omuaran, Kwara State for providing the facilities required to complete this research study.

References

- [1] T. Gutu, "A study on the mechanical strength properties of bamboo to enhance its diversification on its utilization", *International Journal of Innovative Technology and Exploring Engineering*, 2013, vol. 2, no. 5, pp. 314–319.
- [2] N. Kaur, S. Saxena, H. Gaur, P. Goyal, "A review on bamboo fiber composites and its applications", in *International Conference on Infocom Technologies and Unmanned Systems (Trends and Future Directions)*, 2017, pp. 843–849, DOI: [10.1109/ICTUS.2017.8286123](https://doi.org/10.1109/ICTUS.2017.8286123).
- [3] N. Neithalath, J. Weiss, J. Olek, "Acoustic performance and damping behavior of cellulose-cement composites", *Cement and Concrete Composites*, 2004, vol. 26, no. 4, pp. 359–370, DOI: [10.1016/S0958-9465\(03\)00020-9](https://doi.org/10.1016/S0958-9465(03)00020-9).
- [4] P. Zakikhani, R. Zahari, M.T. Sultan, D.L. Majid, "Bamboo fiber extraction and its reinforced polymer composite material", *International Journal of Materials and Metallurgical Engineering Journal*, 2014, vol. 8, pp. 54–57, <https://publications.waset.org/search?q=Bamboo+fiber+extraction+and+its+reinforced+polymer+composite+material>.

- [5] S.W. Mumanya, R.B Tait, M.G. Alexander, "Mechanical of Textile Concrete under accelerated aging conditions", *Cement and Concrete Composites*, 2010, vol. 32, no. 8, pp. 580–588, DOI: [10.1016/j.cemconcomp.2010.07.007](https://doi.org/10.1016/j.cemconcomp.2010.07.007).
- [6] B.J. Kim, C. Yi, K.I. Kang, "Microwave curing of alkali-activated binder using hwangtoh without calcinations", *Construction and Building Materials*, 2015, vol. 98, pp. 465–475, DOI: [10.1016/j.conbuildmat.2015.08.119](https://doi.org/10.1016/j.conbuildmat.2015.08.119).
- [7] *EN 494 Fiber-cement profiled sheets and fittings for roofing-Product specification and test methods*. European Committee for Standardization, BSI- British Standard Institution, London, UK, 1994.
- [8] *ASTM C109 Standard test methods for compressive strength of hydraulic cement mortars (using 50-mm cube specimens)*. 2008.
- [9] *ASTM D1037 Standard test methods for evaluating properties of wood-base fiber and particle panel materials*. 2012.
- [10] G.N. Shete, K.S.U. Upase, "Evaluation of Compressive strength and water absorption of styrene Butadiene Rubber (SBR) latex modified concrete", *International Journal of Emerging Trends in Science & Technology*, 2014, vol. 3, no. 2, pp. 1404–1410.
- [11] T. Chen, W. Liu, R. Qiu, "Mechanical properties and water absorption of hemp fiber-reinforced unsaturated polymer composites: Effect of fiber surface treatment with a hetero functional monomer", *Bio Resources*, 2013, vol. 8, no. 2, pp. 2780–2791.
- [12] B.A. Akinyemi, T. E. Omoniyi, "Effect of moisture on thermal properties of acrylic polymer modified mortar reinforced with alkali treated bamboo fiber", *Journal of the Indian Academy of Wood Science*, 2018, vol. 15, no. 1, pp. 45–51, DOI: [10.1007/s13196-018-0207-4](https://doi.org/10.1007/s13196-018-0207-4).
- [13] O. Adekomaya, K. Adama, "Investigating water absorption and thickness swelling tendencies of polymeric composite materials for external wall application in refrigerated vehicles", *Africa Journal Online*, 2018, vol. 37, no. 1, pp. 1–10, DOI: [10.4314/njt.v37i1.22](https://doi.org/10.4314/njt.v37i1.22).
- [14] Y. Kong, P. Wang, S. Liu, Z. Gao, M. Rao, "Effect of microwave curing on the hydration properties of cement-based material containing glass powder", *Construction and Building Material*, 2018, vol. 158, pp. 563–573, DOI: [10.1016/j.conbuildmat.2017.10.058](https://doi.org/10.1016/j.conbuildmat.2017.10.058).
- [15] M. Ballesteros, J.M. Oliva, M.J. Negro, P. Maanzanares, I. Ballesteros, "Ethanol from lignocelluloses material by a simultaneous saccharification and fermentation process (SFS)", *Process Biochemistry*, 2004, vol. 39, no. 12, pp. 1843–1848, DOI: [10.1016/j.procbio.2003.09.011](https://doi.org/10.1016/j.procbio.2003.09.011).
- [16] B.A. Akinyemi, A. Bamidele, E. Joel, "Response of coir fiber reinforced cement composites to water repellent chemical additive and microwave accelerated curing", *Cellulose*, 2019, vol. 26, no. 8, pp. 4987–4999.
- [17] C.O. Mgbemena, D. Li, M.F. Lin, P.D. Liddel, K.B. Katnam, V.K. Thakur, H.Y. Nezhad, "Accelerated microwave curing of fiber-reinforced thermoset polymer composites for structural applications: A review of scientific challenges. Composites Part A", *Applied Science and Manufacturing*, 2018, vol. 115, no. 3, pp. 88–103, DOI: [10.1016/j.compositesa.2018.09.012](https://doi.org/10.1016/j.compositesa.2018.09.012).
- [18] J.N. Teixeira, D.W. Silva, A.P. Vilela, H.S. Junior, L.E. Brandao, R.F. Mendes, "Lignocellulosic material for fiber cement production", *Waste and Biomass Valorization*, 2020, vol. 11, no. 5, pp. 2193–2200, DOI: [10.1007/s12649-018-0536-y](https://doi.org/10.1007/s12649-018-0536-y).
- [19] N. Makul, P. Rattanadecho, D.K. Agrawal, "Applications of microwave energy in cement and concrete-a review", *Renewable and Sustainable Energy Reviews*, 2014, vol. 37, pp. 715–733, DOI: [10.1016/j.rser.2014.05.054](https://doi.org/10.1016/j.rser.2014.05.054).
- [20] O. Guven, S.N. Monteiro, E.A. Moura, J.W. Drelich, "Re-emerging field of lignocellulosic fiber –polymer composites and ionizing radiation technology in their formulation", *Polymer Reviews*, 2016, vol. 56, no. 4, pp. 702–736, DOI: [10.1080/15583724.2016.1176037](https://doi.org/10.1080/15583724.2016.1176037).
- [21] H. Hajiha, M. Sain, L.H. Mei, "Munification and characterization of hemp and sisal fiber", *Journal of Natural Fibers*, 2014, vol. 11, no. 2, pp. 144–168, DOI: [10.1080/15440478.2013.861779](https://doi.org/10.1080/15440478.2013.861779).
- [22] H.Y. Nezhad, P.D. Liddel, V. Marchante, R. Roy, "A novel process-linked assembly failure model for adhesively bonded composites structures", *CIRP Annals*, 2017, vol. 66, no. 1, pp. 29–32, DOI: [10.1016/j.cirp.2017.04.103](https://doi.org/10.1016/j.cirp.2017.04.103).

- [23] D. Abliz, Y. Duan, X. Zhao, D. Li, “Low –energy electron beam cured tape placement for out –of-autoclave fabrication of advanced polymer composites”, *Applied Science Manufacturing*, 2014, vol. 65, pp. 73–82, DOI: [10.1016/j.compositesa.2014.06.004](https://doi.org/10.1016/j.compositesa.2014.06.004).
- [24] K.F. Adekunle, “Surface treatments of natural fiber”, *Open Journal of Polymer Chemistry*, 2015, vol. 5, no. 3, pp. 41–46, DOI: [10.4236/ojchem.2015.53005](https://doi.org/10.4236/ojchem.2015.53005).
- [25] M. Ardanuy, J. Claramunt, R.D.T. Filho, “Cellulosic fiber reinforced cement- based composites: A review of recent research”, *Construction and Building Materials*, 2015, vol. 79, pp. 115–128, DOI: [10.1016/J.CONBUILDMAT.2015.01.035](https://doi.org/10.1016/J.CONBUILDMAT.2015.01.035).
- [26] A.A. Alaa, B.H.F. Saad, S.K. Ahmed, “High Performance Concrete Improvement by Styrene-Butadiene Rubber Addition”, *Engineering and Technical Journal*, 2016, vol. 34, no. 1, pp. 2296–2309.
- [27] Z. Zuo, J. Zhang, B. Li, C. Shen, G. Xin, X. Chen, “Effect of Curing Regime on the Mechanical Strength, Hydration, and Microstructure of Ecological Ultrahigh-Performance Concrete (EUHPC)”, *Materials*, 2022, vol. 15, art. ID 1668, pp. 1–19, DOI: [10.3390/ma15051668](https://doi.org/10.3390/ma15051668).
- [28] J. Xiao, W. Jiang, D. Yuan, A. Sha, Y. Huang, “Effect of styrene–butadiene rubber latex on the properties of modified porous cement-stabilized aggregate”, *Road Materials and Pavement Design*, 2018, vol. 19, no. 7, pp. 1702–1715, DOI: [10.1080/14680629.2017.1337042](https://doi.org/10.1080/14680629.2017.1337042).

Received: 23.02.2022, Revised: 17.03.2022